IOP Publishing Journal of Geophysics and Engineering
J. Geophys. Eng. 14 (2017) 212–225 (14pp) doi:10.1088/1742-2140/14/2/212

An integrated petrophysical and rock physics analysis to improve reservoir characterization of Cretaceous sand intervals in Middle Indus Basin, Pakistan

Tahir Azeem[1,2], Wang Yan Chun[2], MonaLisa[1], Perveiz Khalid[3], Liu Xue Qing[2], Muhammad Irfan Ehsan[3], Muhammad Jawad Munawar[4] and Xie Wei[2]

[1] Department of Earth Sciences, Quaid-I-Azam University, Islamabad, Pakistan
[2] School of Geophysics and Information Technology, China University of Geosciences, Beijing 100083, People's Republic of China
[3] Institute of Geology, University of the Punjab, 54590 Lahore, Pakistan
[4] School of Geosciences, China University of Petroleum, Qingdao, People's Republic of China

E-mail: tahir2rd@yahoo.com

Received 15 October 2015, revised 24 November 2016
Accepted for publication 30 November 2016
Published 20 January 2017

Abstract

The sand intervals of the Lower Goru Formation of the Cretaceous age, widely distributed in the Middle and Lower Indus Basin of Pakistan, are proven reservoirs. However, in the Sawan gas field of the Middle Indus Basin, these sandstone intervals are very deep and extremely heterogeneous in character, which makes it difficult to discriminate lithologies and fluid saturation. Based on petrophysical analysis and rock physics modeling, an integrated approach is adopted to discriminate between lithologies and fluid saturation in the above-mentioned sand intervals. The seismic velocities are modeled using the Xu–White clay–sand mixing rock physics model. The calibrated rock physics model shows good consistency between measured and modeled velocities. The correlation between measured and modeled *P* and *S* wave velocities is 92.76% and 84.99%, respectively. This calibrated model has been successfully used to estimate other elastic parameters, even in those wells where both shear and sonic logs were missing. These estimated elastic parameters were cross-plotted to discriminate between the lithology and fluid content in the target zone. Cross plots clearly separate the shale, shaly sand, and gas-bearing sand clusters, which was not possible through conventional petrophysical analysis. These data clusters have been exported to the corresponding well for the purpose of interpolation between wells and to analyze the lateral and vertical variations in lithology and fluid content in the reservoir zone.

Keywords: petrophysics, rock physics modeling, elastic parameters, reservoir characterization, cross well correlation, Sawan gas field

(Some figures may appear in colour only in the online journal)

1. Introduction

Petrophysical analysis plays an important role in reservoir characterization, especially in discriminating between the hydrocarbon and non-hydrocarbon bearing zones (Yuedong and Hongwei 2007). In the literature, different techniques have been proposed for fluid and lithology discrimination (Castagna and Swan 1997, Chi and Han 2009, He *et al* 2011, Hu *et al* 2011, Ahmed *et al* 2016). Generally, petrophysical analysis is performed to transform the wireline log data into

reservoir properties such as volume of shale, porosity, permeability, and water and hydrocarbon saturation. Proper analysis of these reservoir properties can significantly enhance the ability to discriminate between the hydrocarbon and non-hydrocarbon bearing zones (Ajisafe and Ako 2013). However, petrophysical results can be affected by bad borehole conditions, missing logs, temperature, pressure, and salinity. In addition, based on single-well data, petrophysical models are generally established for the particular interval of interest. Therefore, petrophysical models are often consistent over the particular interval of the well and sometimes fail to provide good results between the wells, even when the wells are very closely spaced (Bisht *et al* 2013). The integrated workflows of petrophysics and rock physics are used to find a consistent rock physics model for the entire area of interest. Once a consistent rock physics model has been established, it can be effectively used to synthesize the elastic logs, identify the inconsistencies in the well logs and quick well data analysis, and improve seismic to well tie, which improves the reservoir characterization and minimizes the risk of uncertainty (Bisht *et al* 2013, Sams 2014). These calibrated models also have the ability to accurately predict the variations in lithology and fluid saturation (Odegaard and Avseth 2004, Mavko *et al* 2009, Grana *et al* 2012). The most important aspect of these integrated models is to use the accurate and consistent mineral and fluid properties, which leads to an accurate calibration of these rock physics models (Mavko *et al* 2009). Accurate and consistent rock physics models not only efficiently differentiate between the hydrocarbon- and non-hydrocarbon-bearing zones but also indicate the problems present in the well log data such as borehole washouts, data gaps, mud filtrate, and insufficient log suites (Avseth *et al* 2001).

Integrated rock physics models provide more accurate and reliable links between petrophysics and seismic and reservoir properties (Avseth 2000, Xu and Payne 2009, He *et al* 2011, Khalid *et al* 2014b). A significant number of rock physics models have been proposed by various workers (Mavko *et al* 2009). Avseth *et al* (2005) has classified these models into different categories such as inclusion models (Kuster and Toksoz 1974, Cheng and Toksöz 1979, Berryman 1980, Liu and Sun 2015), contact models (Mindlin 1949, Walton 1987, Dvorkin *et al* 1994, Dvorkin and Nur 1996), transformations (Gassmann 1951, Berryman and Milton 1991), bounds (Voigt 1910, Reuss 1929, Hill 1952, Hashin and Shtrikman 1963), and computational models. Recently, Khalid *et al* (2014) proposed a modified rock physics model based on thermodynamic properties of reservoir fluids at *in situ* conditions.

Inclusion models ponder the rock as an elastic block of minerals containing the pore spaces. Therefore, results of these models show better consistency with the measured well log data. Xu and White (1995) proposed a clay–sand mixture model which is based on the Kuster and Toksoz (1974) inclusion model, supplemented by the Gassmann (1951) and effective medium theories (Zhang 2008). This model can account for the effect of clay content on the seismic velocities, and is very useful for estimating shear wave velocity. A combination of shear and acoustic velocities has been extensively used as a seismic attribute in reservoir characterization (Avseth *et al* 2005, Chi and Han 2009). Seismic velocities of rock provide information about minerals, pore fluids, and their distribution within the rock skeleton (Mavko *et al* 1998, Avseth 2000, Feng-Ying *et al* 2014). Like other parameters such as porosity, permeability, fluid saturation, fluid composition, formation temperature, pressure, and mineralogy, clay content also influences the seismic properties of a porous rock (Ahmed *et al* 2016, Wang *et al* 2015). The presence of clay decreases the seismic velocities (Minear 1982, Han *et al* 1986, Marion *et al* 1992, Ahmed *at al* 2016) and aspect ratio values (Sams and Andrea 2001, Sams and Focht 2013). Thus, it is important to account for the volume and distribution of clay when trying to estimate the elastic velocities.

The Lower Goru Formation of the Cretaceous age is a proven reservoir in the middle and lower Indus Basin of Pakistan. In the Sawan gas field of the middle Indus Basin, the sand intervals of this formation are composed of quartz, feldspar, volcanic rock fragments, chlorite, clay, glauconite, and minor amounts of calcite. The core and wireline log data show that the mineral composition of these sands is very much heterogeneous from one well to another, which makes it difficult to use a single petrophysical model for reservoir characterization. The aim of this study is to use an integrated approach based on petrophysical analysis and a rock physics model to solve the rock heterogeneity effects (Fitch *et al* 2015, Ahmed *et al* 2016, Khalid *et al* 2016) on seismic properties such as velocities and elastic moduli of the sand intervals. The rock physics model proposed by Xu and White (1995) is calibrated using wireline logs for the study area.

2. Geological setting

The study area is located in the north–south trending prolific middle Indus Basin, which is bounded by the Indian shield in the east; Kirther Ranges, Sulaiman Fold, and Thrust Belt in the west; Sargodha High in the north; and Jacobabad–Khairpur High in the south (Kadri 1995). The location of the study area and Jacobabad High is shown in figure 1. In the northwest direction of the study area, the famous Khairpur High is located that exhibits very high geothermal gradient up to 4.8 °C/100 m. Khairpur High played an important role in the formation of structural traps in the Kadanwari, Sawan, and surrounding areas (Ahmad and Chaudhry 2002, Berger *et al* 2009). Since the Indus Basin is rich in hydrocarbon and contains several complete petroleum systems, a large number of wells have been drilled in the middle and lower Indus Basin. The organic rich black shales of the Sembar Formation, early Cretaceous in age, are the proven primary source rock in the basin. In the middle and lower Indus Basin, the Sembar Formation, with variable thickness (0–260 m), has been deposited in a marine environment (Iqbal and Shah 1980). Sembar Formation mainly consists of type-III kerogen organic matter, which is mainly favorable for gas generation. This formation is deeper and thermally mature

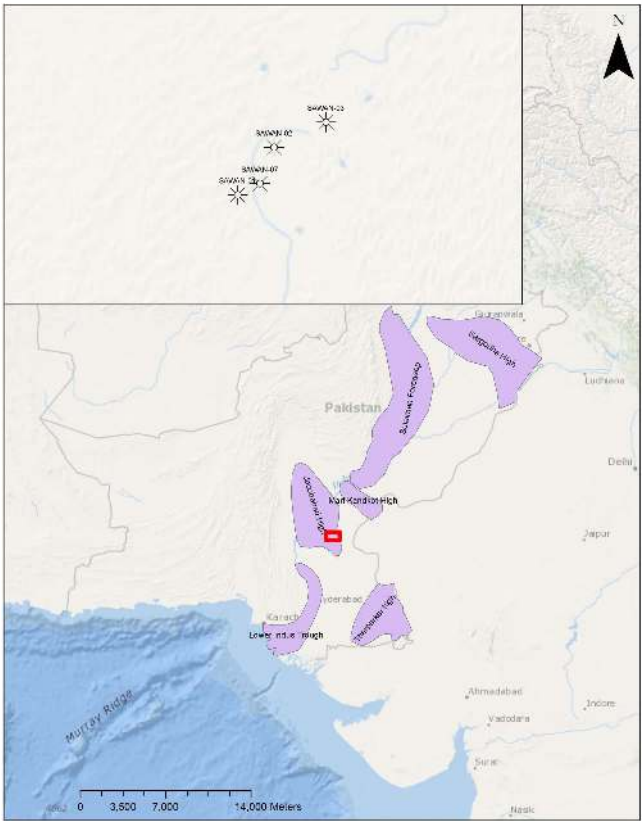

Figure 1. Location of the study area and other prominent geological features.

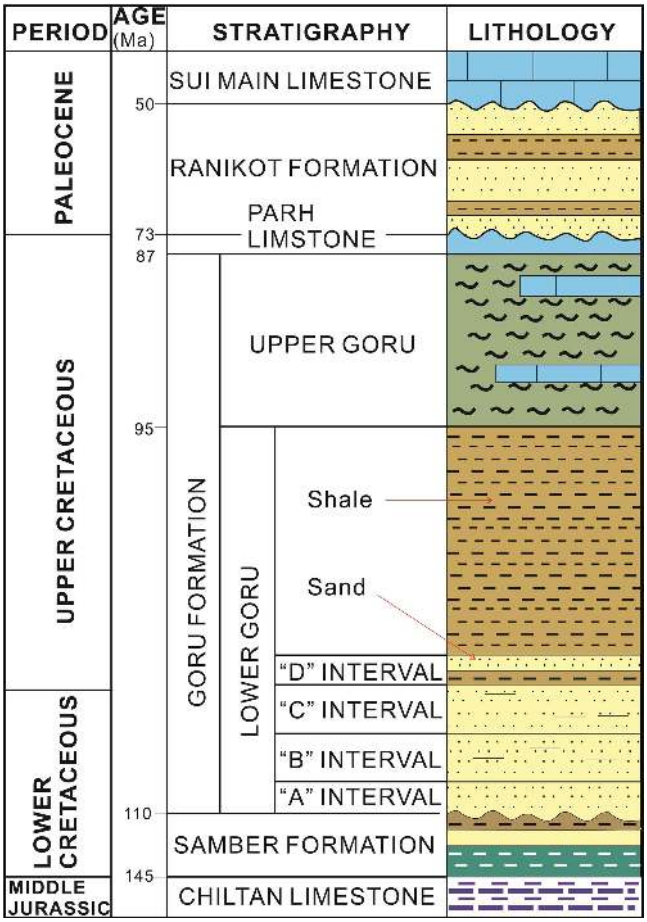

Figure 2. Generalized stratigraphic column showing sand and shale distribution in the Lower Goru Formation (modified after Krois *et al* 1998. Reproduced with permission from Pakistan Association of Petroleum Geologists Islamabad).

towards the western part, while it is shallower and less mature towards the eastern part of the Indus Basin (Wandrey *et al* 2004). Sembar Formation is overlain by the Goru Formation, which is divided into two parts. The upper part is mainly composed of shale and is termed the Upper Goru whereas the lower part is termed the Lower Goru (Kadri 1995).

The medium to coarse grained sandstone of the Lower Goru Formation is the main reservoir rock in the middle Indus Basin, which is deposited in a shallow marine environment. This reservoir formation is composed of sandstone, siltstone, inter-bedded shale, and thin bedded limestone (Kazmi and Jan 1997, Berger *et al* 2009). The lower sandy part of this formation has been further divided (from bottom to top) into four stratigraphic intervals, i.e., A, B, C, and D as shown in figure 2 (Krois *et al* 1998). The B, C, and D intervals act as potential gas reservoirs in the study area (Ahmad *et al* 2004, Munir *et al* 2011). Petrographic analysis reveals that the A and B intervals are quartz arenite, whereas the C interval is sublithic to lithic arenite, which includes a significant amount (almost 13%) of partially altered basic volcanic rock fragments (McPhee and Enzendorfer 2004, Berger *et al* 2009). The upper part of the Lower Goru Formation acts as a regional seal which is mainly composed of transgressive, siderite cemented shales and siltstones. Chlorite acts as cement and comprises almost 80% of the clay fraction; this significant amount of the chlorite decreases the porosity of the rocks (McPhee and Enzendorfer 2004).

3. Methodology

The sand intervals of the Lower Goru Formation in the Sawan gas field are very heterogeneous, are considered as hot sands, and reflect a high value of gamma ray and sonic logs, which makes it complicated to accurately estimate the reservoir zones through conventional petrophysical analysis. The reservoir exhibits high temperature (175 °C) and pressure (37.14 MPa) due to high geothermal gradient and burial depth. Wireline logs (e.g., DT, GR, SP, RHOB, NPHI, LLD, LLS, and LLS) from four wells (Sawan-01, 02, 03 and 07) were used for this study. Well Sawan-07 has a full suite of logs and the borehole condition also seems to be good in the target zone. In other wells, shear log is missing and borehole conditions in the target zone are also not as good as in the Sawan-07 well. Log data from the Sawan-07 well along with mineral and fluid properties have been used to calibrate the Xu–White (1995) rock physics model. The workflow of the methodology is shown in figure 3. In the first step, the petrophysical parameters of the reservoir intervals are estimated using PowerLog software. Volume of shale, effective porosity, and water saturation parameters have been estimated by using the available well log data set through petrophysical

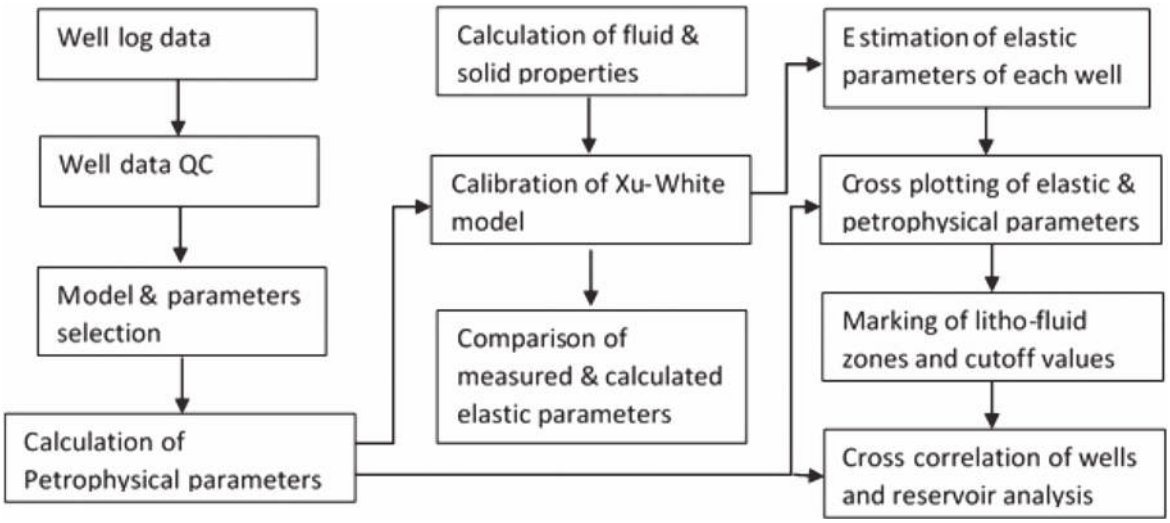

Figure 3. Schematic diagram of the technique used for improved reservoir characterization.

analysis. In a second step, these estimated petrophysical parameters along with fluid properties, solid mineral matrix values, and pore aspect ratios were utilized to calibrate the proposed model. Then, modeled and measured velocities were cross-plotted to check the degree of matching. In next step, this calibrated model was used to estimate elastic parameters in the remaining available wells. These estimated elastic parameters have been cross-plotted to mark the litho-fluid zones and cutoff values of each elastic and petrophysical parameter. Finally, correlation between wells was performed to check the lateral and vertical variations in the target zone.

4. Results and discussion

The methodology proposed in the previous section is applied on the wireline logs of four wells: Sawan-01, -02, -03, and -07. In this section, the petrophysical study of reservoir intervals is presented firstly. Then the results of rock physics modeling are thoroughly discussed. The calibrated rock physics model and petrophysical analysis are used for reservoir characterization in the reservoir intervals encountered in the four wells of the study area.

4.1. Petrophysical analysis

Petrophysical analysis fills a gap between core and seismic data and plays an important role in reservoir characterization. The estimation of various petrophysical parameters from wireline logs with accuracy can significantly enhance the ability to interpret the lithology and reservoir characterization (Fitch *et al* 2015). The quality of log data has a strong influence on the accuracy of rock physics models (Avseth *et al* 2001). Conventional well log curves such as density, gamma ray, caliper, resistivity, neutron porosity, and sonic are available in the Sawan-07 well. Considering the availability of well log curves and borehole conditions, the Sawan-07 well was chosen as a reference well for this study. Petrophysical parameters such as volume of shale, effective porosity, and water saturation were estimated as follows.

4.1.1. Volume of shale. Proper estimation of shale content provides the basis for accurately deriving the other petrophysical parameters such as porosity and water saturation in the shaly formation. Different shale indicator methods are used in practice, which are based on the estimation of gamma ray index (equation (1)) from the gamma ray log:

$$I_{GR} = \frac{GR_{\log} - GR_{\min}}{GR_{\max} - GR_{\min}}, \tag{1}$$

where I_{GR} is gamma ray index. $GR_{\log}$ represents gamma ray log value at a particular depth, while $GR_{\min}$ and $GR_{\max}$ are minimum and maximum values of gamma ray log in a given depth interval. However, this linear method overestimates the volume of shale in real formations (Poupon and Gaymard 1970), whereas non-linear methods give more accurate results (Larionov 1969, Stieber 1970, Clavier *et al* 1971). Therefore, we have used these non-linear methods to estimate the volume of shale (equations (2)–(4)). The value of I_{GR} has been substituted in equations (2)–(4) to estimate the volume of shale:

$$V_{\mathrm{sh(Larionov\_old)}} = 0.33(2^{(2\times I_{GR})} - 1) \tag{2}$$

$$V_{\mathrm{sh(Stieber)}} = \frac{I_{GR}}{3-2\times I_{GR}} \tag{3}$$

$$V_{\mathrm{sh(Clavier)}} = 1.7\sqrt{3.38 - (I_{GR} + 0.7)^2}\,. \tag{4}$$

Here, $V_{\mathrm{sh(Larionov\_old)}}$, $V_{\mathrm{sh(Stieber)}}$, and $V_{\mathrm{sh(Clavier)}}$ represent volume of shale measured using Larionov old rock, Stieber, and Clavier methods, respectively. The estimated shale volumes are shown in figure 4. The purpose of using different methods was to choose the method which gives lowest volume of shale in order to minimize the risk of errors due to the presence of hot sands (sands including some content of radioactive material, usually potassium or thorium, and

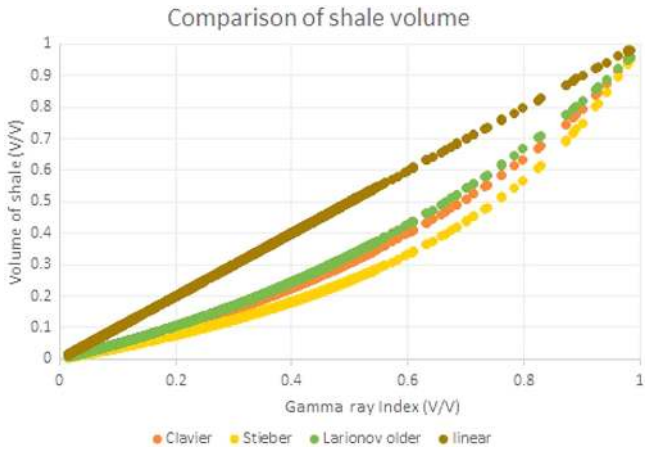

Figure 4. Cross plot between gamma ray index and volume of shale calculated by different methods.

showing high values of gamma ray log) or interbedded shales (Hussein and Ahmed 2012). In practice, the neutron-density method is used to minimize the effect of radioactive minerals. However, in some cases, the neutron-density method does not provide accurate results, especially when hot sand is saturated with gas or light hydrocarbon fluids (Hamada 1996, Adeoti *et al* 2009). In the case of dirty sand, modern spectral gamma ray is a more appropriate technique for computing volume of shale. Since spectral gamma ray was not available, non-linear methods proposed by different authors (Larionov 1969, Stieber 1970, Clavier *et al* 1971) were used to calculate the volume of shale of the target interval. Figure 4 clearly indicates that the volume of shale calculated using the Stieber (1970) method is lower compared to other methods. Moreover, the Stieber method is also suitable for gas reservoirs (Adeoti *et al* 2009). Therefore, volume of shale calculated by using the Stieber method was utilized for further analysis.

4.1.2. Porosity. Gas saturation near the wellbore affects the porosity logs. In the gas-bearing zone the density porosity log shows high values whereas the neutron porosity log shows low values, so a combination of neutron and density porosities is used to remove this effect. However, in shaly formation, it is necessary to remove the effect of shale as the presence of shale affects the porosity. Equations (5) and (6) were used to remove the effect of shale on neutron and density porosities (Schlumberger 1974, Doveton 1999):

$$\Phi_{NC} = \Phi_N - V_{sh}\Phi_{Nsh}, \quad (5)$$

$$\Phi_{DC} = \Phi_D - V_{sh}\Phi_{Dsh}, \quad (.6)$$

Here, Φ_{NC} and Φ_{DC} are the corrected neutron and density porosities; Φ_N and Φ_D represent neutron and density porosity log, respectively; while Φ_{Nsh} and Φ_{Dsh} represent neutron and density porosities in the shaly area, respectively. Finally, we combined these corrected porosities in order to calculate the effective porosity Φ_e:

$$\Phi_e = \sqrt{\frac{(\Phi_{NC})^2 + (\Phi_{DC})^2}{2}}. \quad (7)$$

4.1.3. Water saturation. As the presence of shale also affects the water saturation, we compensate for the effect of shale by applying the Indonesian model (Poupon and Levaux 1971). This model improves the results reliability in shaly formations, as it is based on field observations (Widarsono 2012, Alao *et al* 2013). The mathematical form of this model is

$$S_w = \left[\left\{\left(\frac{V_{sh}^{2-V_{sh}}}{R_{sh}}\right)^{1/2} + \left(\frac{\phi_e^m}{R_w}\right)^{1/2}\right\}^2 R_t\right]^{-1/2}, \quad (8)$$

where S_w represents water saturation; R_{sh}, R_w, and R_t are the shale, water, and true resistivities, respectively; m is cementation factor and its value is 2.15; V_{sh} is volume of shale; and ϕ_e is effective porosity. These estimated petrophysical parameters (volume of shale, porosity, and water saturation) are shown in figure 5.

4.2. Rock physics modeling/calibration of rock physics model

Rock physics modeling is a process of finding an appropriate model that shows good consistency with the available well log data (Walls *et al* 2004). The proposed Xu–White (1995) clay–sand mixing model is based on the Kuster and Toksoz (1974) model supplemented by the Gassmann (1951) and pore aspect ratio theories. This model has the ability to separate the sand- and clay-related pores by assigning them different aspect ratios. If α_S and α_c are the aspect ratios of sand- and clay-related pores, Φ_S and Φ_c are porosities of sand grains and clay content, respectively. Then these sand and clay grains can be mixed through clay content in order to calculate the elastic properties of dry rock porous media, as shown in equations (9)–(11):

$$\frac{K_d - K_m}{3K_d + 4\mu_m} = \frac{1}{3}\left(\frac{K_f - K_m}{3K_m + 4\mu_m}\right)\sum_{l=s,c}\Phi_l T_{iijj}(\alpha_l), \quad (9)$$

$$\frac{\mu_d - \mu_m}{6\mu_d(K_m + 2\mu_m) + \mu_m(9K_m + 8\mu_m)} = \frac{\mu_f - \mu_m}{25\mu_m(3K_m + 4\mu_m)}\sum_{l=s,c}\Phi_l F(\alpha_l), \quad (10)$$

$$F(\alpha_l) = T_{iijj}(\alpha_l) - \frac{T_{ijij}(\alpha_l)}{3}, \quad (11)$$

where K_d, K_m, and K_f represent bulk modulus of dry rock frame, solid matrix, and pore fluid respectively, and μ_d, μ_m, and μ_f represent the corresponding shear modulus. Φ is the porosity, while $Tiijj(\alpha_l)$ and $Tijij(\alpha_l)$ are the scalar functions of the aspect ratio, which have been calculated using the Eshelby (1957) approach.

The elastic properties of clay are not well established in this area and vary dramatically for different clay types. At the initial stage of this model, we used the typical solid mineral values for clay and sand as proposed by Han *et al* (1986) and

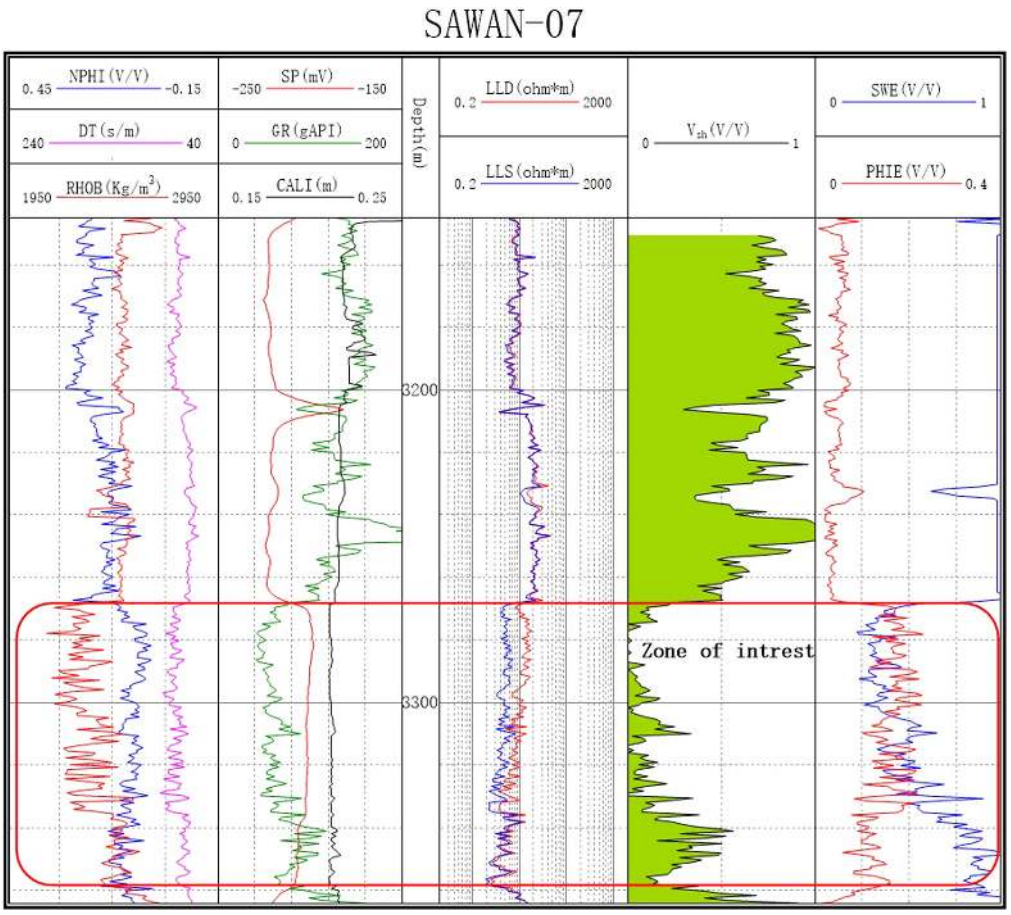

Figure 5. Display of log curves and estimated petrophysical parameters in the Lower Goru Formation encountered in the Sawan-07 well.

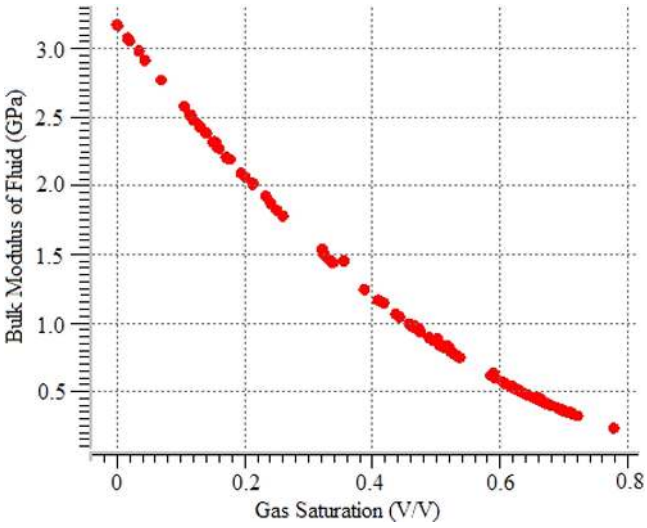

Figure 6. Analysis of gas saturation versus bulk modulus of fluid estimated using Brie's fluid-mixing algorithm.

Table 1. Parameters used for rock physics modeling.

Parameters	Symbols	Numerical Value	Units
Bulk modulus of sand	K_s	3.7×10^{10}	Pa
Shear modulus of sand	μ_s	4.4×10^{10}	Pa
Density of sand	ρ_s	2650	Kg m^{-3}
Bulk modulus of clay	K_c	2.14×10^{10}	Pa
Shear modulus of clay	μ_c	1.19×10^{10}	Pa
Density of clay	ρ_c	2590	Kg m^{-3}
Reservoir temperature	T	448	K
Reservoir pressure	P	37.14	MPa
Salinity of brine	S_b	20 000	ppm
Specific gravity of gas	G_{gas}	0.642	SG
Bulk modulus of gas	K_g	7.97×10^7	Pa
Density of gas	ρ_g	171.23	Kg m^{-3}
Bulk modulus of brine	K_b	3.17×10^9	Pa
Density of brine	ρ_b	928.18	Kg m^{-3}
Aspect ratio of sand	α_S	0.12	Unitless
Aspect ratio of shale	α_C	0.035	Unitless

Carmichael (1989), respectively. The Wyllie *et al* (1956) time average equation was used as a mixing algorithm to get the solid matrix properties. Batzle and Wang (1992) proposed relationships were used to compute *in situ* fluid temperature and pressure. These fluid properties have been mixed using the Brie *et al* (1995) mixing algorithm as shown in equation (12):

$$K_{\text{Brie}} = (K_b - K_g)(S_w)^e + K_g, \quad (12)$$

where S_w represents water saturation; K_b and K_g are the bulk modulus of brine and gas, respectively; K_{Brie} represents the

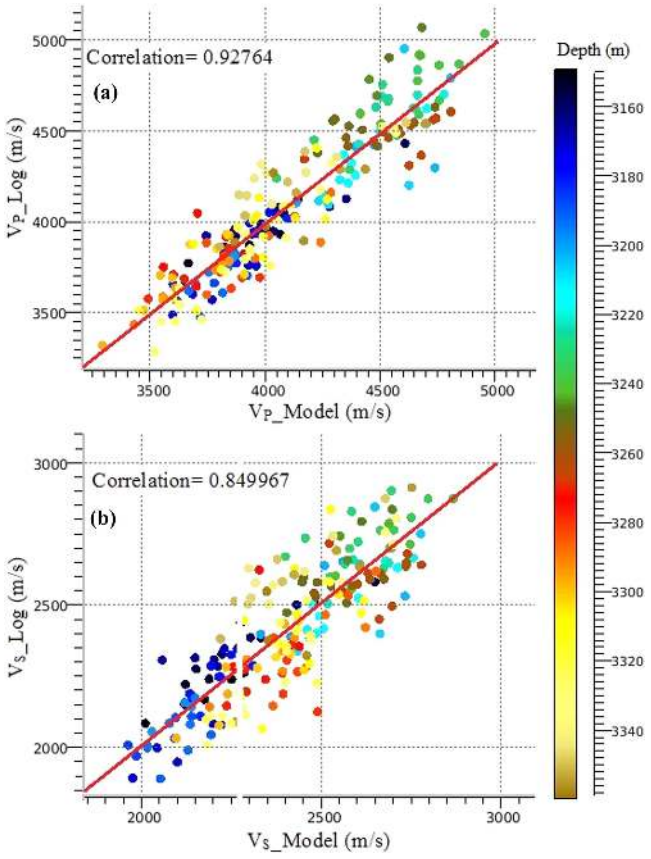

Figure 7. Cross plot between measured and calculated velocities using reference well data (Sawan-07): (a) P-wave velocity, (b) S-wave velocity; color coding represents measured depth.

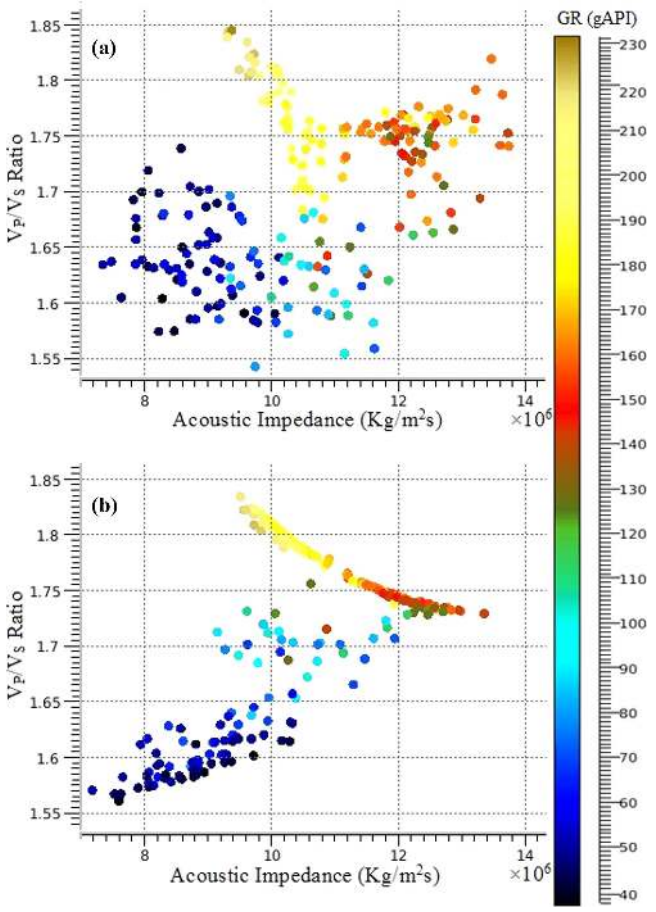

Figure 8. Comparison between measured and modeled elastic properties to check the effectiveness of the model. (a) Measured acoustic impedance versus V_P/V_S ratio. (b) Modeled acoustic impedance versus V_P/V_S ratio. The data points are color coded by gamma ray log.

bulk modulus of fluid calculated using Brie's approach; and e is the exponent of fluid mixing whose value varies from 1 to 40. When $e = 1$, the mixing is Voigt's average and when $e = 40$, the mixing results are very near to wood's average (Brie *et al* 1995). Figure 6 clearly shows that the value of fluid modulus (K_{Brie}) increases with decrease in gas saturation (S_g) and vice versa. This behavior indicates that the stiffness of effective modulus of gas-bearing sediments decreases with the increase in gas saturation.

The elastic moduli of saturated rocks were calculated using the Gassmann (1951) fluid substitution model, which gives the relationship between bulk modulus of saturated rock, dry rock modulus, pore fluid, and solid matrix (equations (13) and (14)):

$$K_{\text{sat}} - K_{\text{d}} = \frac{\left(\frac{1 - K_{\text{d}}}{K_{\text{m}}}\right)^2}{\frac{\Phi}{K_{\text{f}}} + \frac{(1 - \Phi)}{K_{\text{m}}} - \frac{K_{\text{d}}}{K_{\text{m}}^2}} \tag{13}$$

$$\mu_{\text{sat}} = \mu_{\text{d}}. \tag{14}$$

Density of saturated rock was calculated using equation (15):

$$\rho_{\text{sat}} = \Phi\rho_{\text{f}} + (1 - \Phi)\rho_{\text{m}}. \tag{15}$$

Here, K_{sat} and μ_{sat} are the bulk and shear modulus of the saturated rocks, respectively, whereas ρ_{sat}, ρ_{f}, and ρ_{m} represent the densities of the saturated rock, pore fluid, and solid matrix, respectively. Finally, we substitute K_{sat}, μ_{sat}, and ρ_{sat} values in equations (16) and (17) to obtain the elastic velocities

$$V_{\text{P}} = \sqrt{\frac{K_{\text{sat}} + \frac{4\mu_{\text{sat}}}{3}}{\rho_{\text{sat}}}} \tag{16}$$

$$V_{\text{S}} = \sqrt{\frac{\mu_{\text{sat}}}{\rho_{\text{sat}}}}. \tag{17}$$

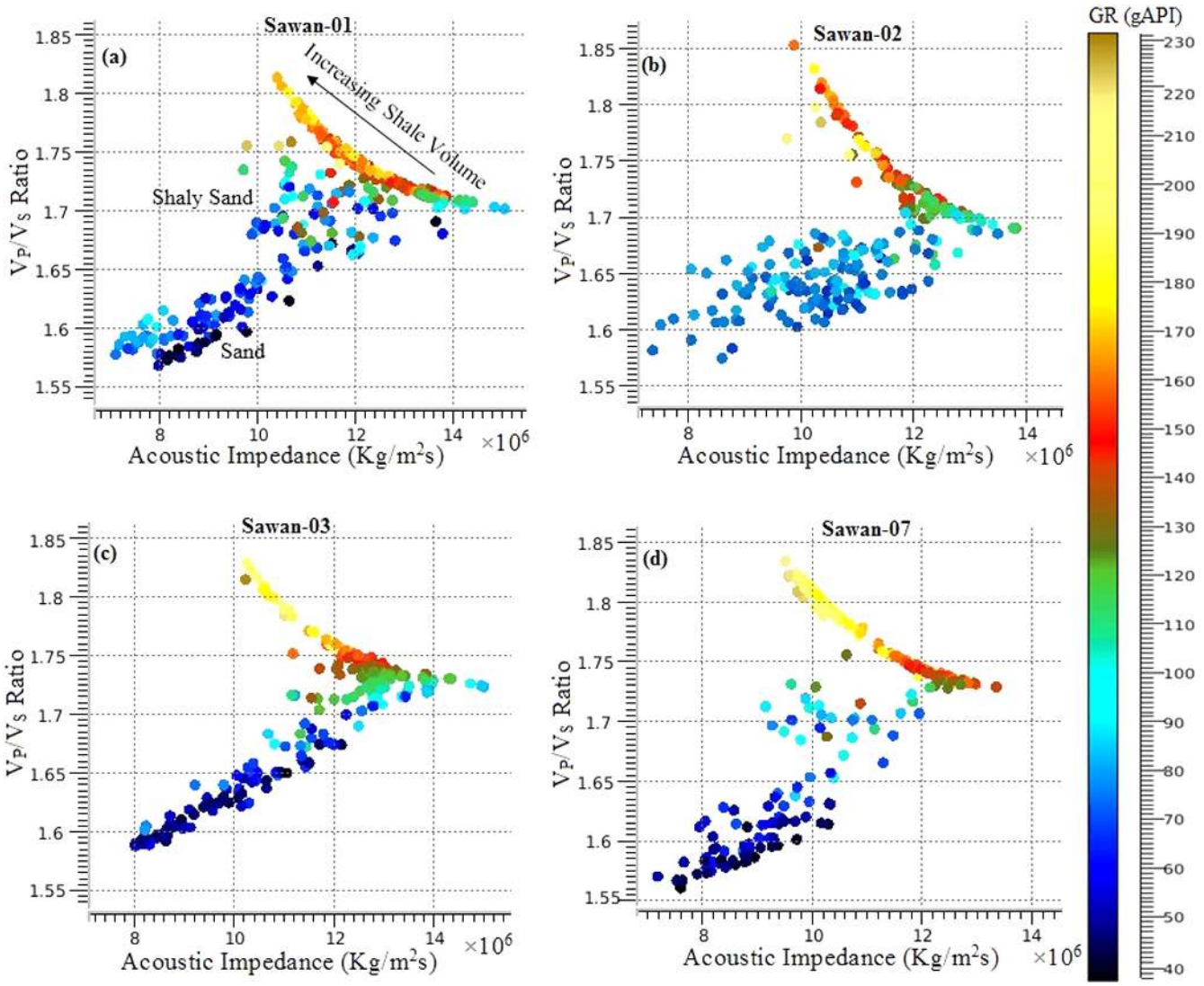

Figure 9. Cross plots of acoustic impedance versus V_P/V_S ratio developed using modeled elastic parameters of (a) Sawan-01, (b) Sawan-02, (c) Sawan-03, and (d) Sawan-07 wells at various gamma ray values.

After building a rock physics model, the most important task is to adjust the input parameters for the specific reservoir. Most of the default parameters failed to properly match the modeled logs with the measured logs, as elastic properties of clay have not been clearly defined. Therefore, it is necessary to adjust the elastic parameters (density, P and S wave velocities) of clay to achieve an optimal fit with the measured logs within the target interval. For this purpose, we constructed a series of models to adjust the elastic values of clay and aspect ratios. The typical values for sand and clay related pores are 0.12–0.15 and 0.02–0.0, respectively (Xu and White 1995) which were tested in the calibration process. We observed that if low values of elastic parameters were chosen, then higher values of aspect ratios were required to achieve a good match between measured and modeled logs. Moreover, the value of aspect ratio decreases with the increase in clay content and decrease in porosity. After trial and error, the final values of aspect ratios and elastic parameters were selected (table 1). At these selected values, the modeled velocities show very good consistency with the measured velocities (figure 7).

4.3. Reservoir characterization

Rock physics models are utilized as an important tool in reservoir characterization. They create the bridge between elastic properties (P-wave velocity, S-wave velocity, density, impedance, and V_P/V_S ratio) and reservoir properties (porosity, permeability, and saturation) (Avseth 2000, Chi and Han 2009). The calibrated rock physics model has been utilized to estimate the elastic properties of reservoir interval encountered in each well. The derived petrophysical parameters from petrophysical analysis are cross-plotted against the elastic properties computed from the rock physics model in the reservoir intervals. Cross-plotting of different parameters is a powerful tool for visual analysis and helpful in marking the data clusters in the target zones (White 1991). Based on their response, these data clusters can be classified into different lithologies/facies (Mavko *et al* 1998). Elastic

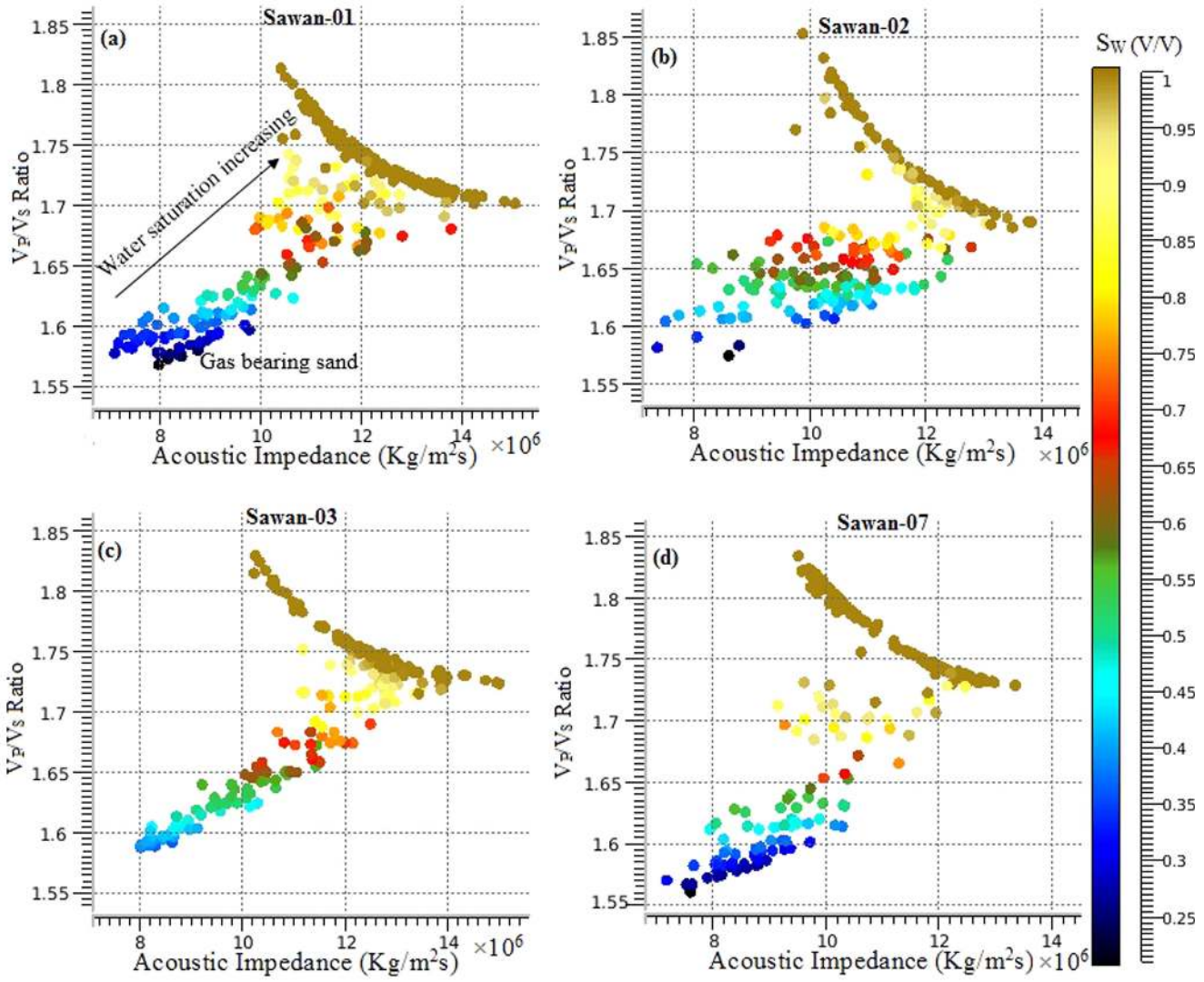

Figure 10. Cross plots of acoustic impedance versus V_P/V_S ratio developed using modeled elastic parameters of (a) Sawan-01, (b) Sawan-02, (c) Sawan-03, and (d) Sawan-07 wells at different water saturation values. Data cluster with low acoustic impedance, V_P/V_S ratio, and water saturation shows gas saturation.

attributes (V_P/V_S ratio) has the ability to discriminate between different type of lithology and payable sand in the target zone (Benzing *et al* 1983, Miller and Stewart 1990, Hughes *et al* 2008). However, a combination of P-impedance and V_P/V_S ratio can be utilized to efficiently predict the lithology and fluid saturation (Odegaard and Avseth 2004, Avseth and Bachrach 2005, Chi and Han 2009).

To verify the effectiveness of the model, calculated and measured elastic impedance is cross-plotted against V_P/V_S ratio for the entire reservoir interval (figure 8). The data points are color coded using gamma ray log. Figures 8(a) and (b) are totally different from each other. The cross plot between modeled parameters (figure 8(b)) clearly separates the different types of facies whereas cross plot between measured (logs) parameters (figure 8(a)) fails to separate these facies. Since the measured log data is affected by different parameters and environmental conditions, it is difficult to discriminate fluid contents or lithology from log data. However, in modeled data, we have more control over the input parameters, so it is more suitable and effective for differentiating different type of facies as shown in figure 8. The facies against high GR values (shales) are clearly separated from the facies of low GR values (sands). Keeping in mind the effectiveness of the model, cross plots between V_P/V_S and acoustic impedance (figure 9) have been developed in order to discriminate between the different type of facies in all wells. In each cross plot (figures 9(a)–(d)), different type of data clusters can be clearly identified in the graphs. The data cluster present at the lower portion of the graph with low acoustic impedance, V_P/V_S ratio, and gamma ray values represents clean sand. However, the upper part of the cross plots, where higher V_P/V_S ratio and gamma ray values are plotted in curve-like form, represent shale. The trends of these parameters are closely matched with the cross plots done by Castagna *et al* (1993). Shaly sand exhibits different behavior than sand and shale, and it can be clearly identified at each cross plot between these two sand and shale bodies. Shaly sand sediments exhibit gamma ray values between 80 to 120

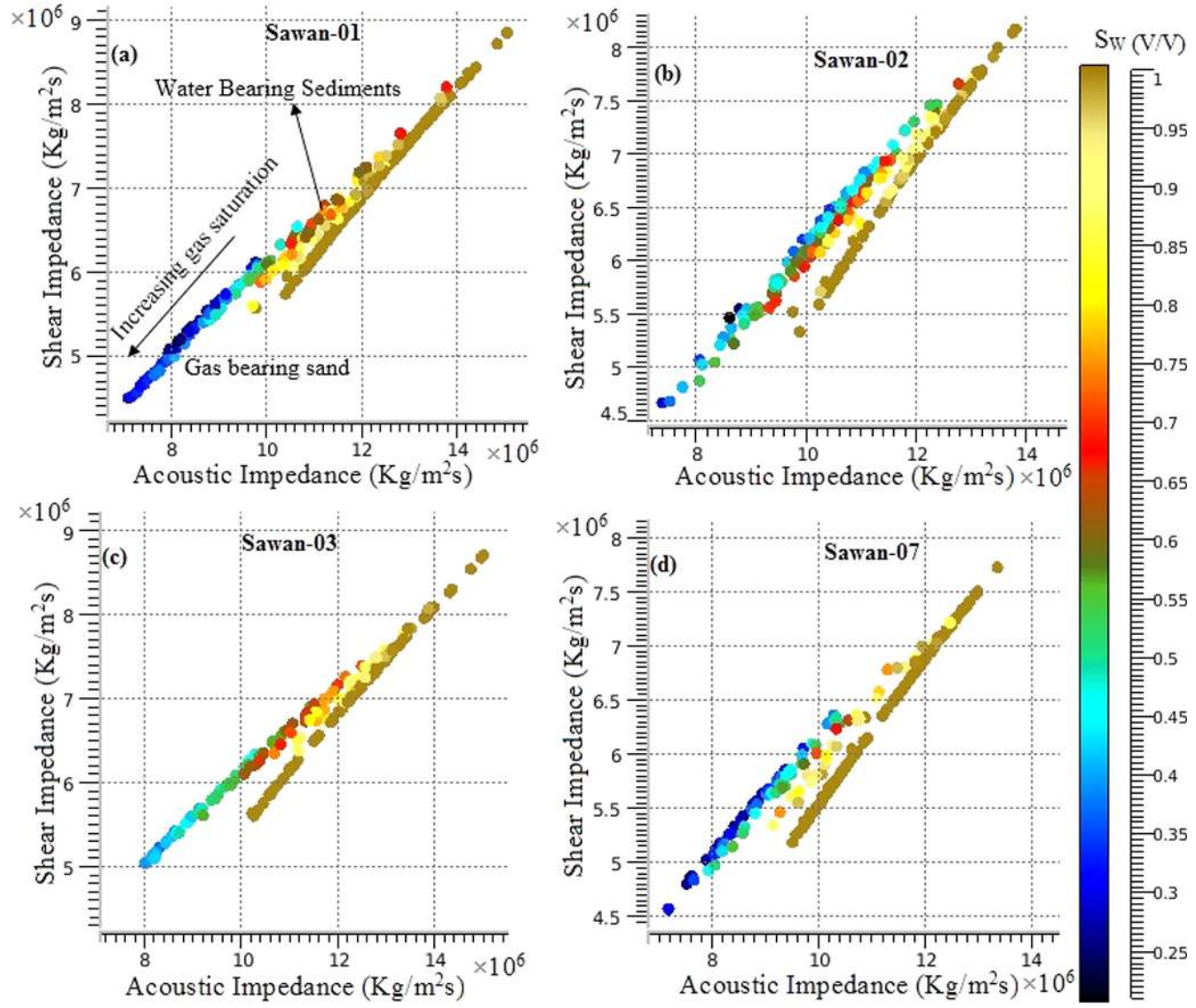

Figure 11. Cross plots of acoustic impedance versus shear impedance calculated using modeled elastic properties of (a) Sawan-01, (b) Sawan-02, (c) Sawan-03, and (d) Sawan-07 wells. Color coding represents water saturation. Data cluster with low water saturation, acoustic impedance, and shear impedance represents gas-saturated zone.

Table 2. Quantitative values (in average) of elastic and petrophysical parameters for different identified rock types.

	Rock Type		
Parameters	Gas-Bearing Sand	Shaly Sand	Shale
Gamma ray (API)	<80	80–120	>120
Water saturation (V/V)	<0.55	0.55–0.9	>0.9
Porosity (V/V)	>0.11	0.05–0.11	<0.05
P-Impedance (Kg m^{-2*}S)	$<1.02 \times 10^7$	1.02×10^7–1.2×10^7	$>1.2 \times 10^7$
S-Impedance(Kg m^{-2*}S)	6.2×10^6	6.2×10^6–7.2×10^6	$>7.2 \times 10^6$
Vp/Vs ratio	⩽1.65	>1.65–1.72	>1.72

API. On the other hand, if sand is saturated with gas, then the value of acoustic impedance, V_P/V_S ratio, and water saturation parameters will be on the lower side (figure 10). The presence of gas strongly affects the elastic parameters and causes the acoustic impedance and V_P/V_S ratio values to decrease (Zhao *et al* 2013). From figures 10(a)–(d), it can be clearly seen that the gas-bearing sediments have V_P/V_S and acoustic impedance values less than or equal to 1.65 and 1.02×10^7, respectively.

Rock physics attributes such as acoustic and shear impedances have been combined to discriminate fluid saturation. Water saturation is used to color code the data points

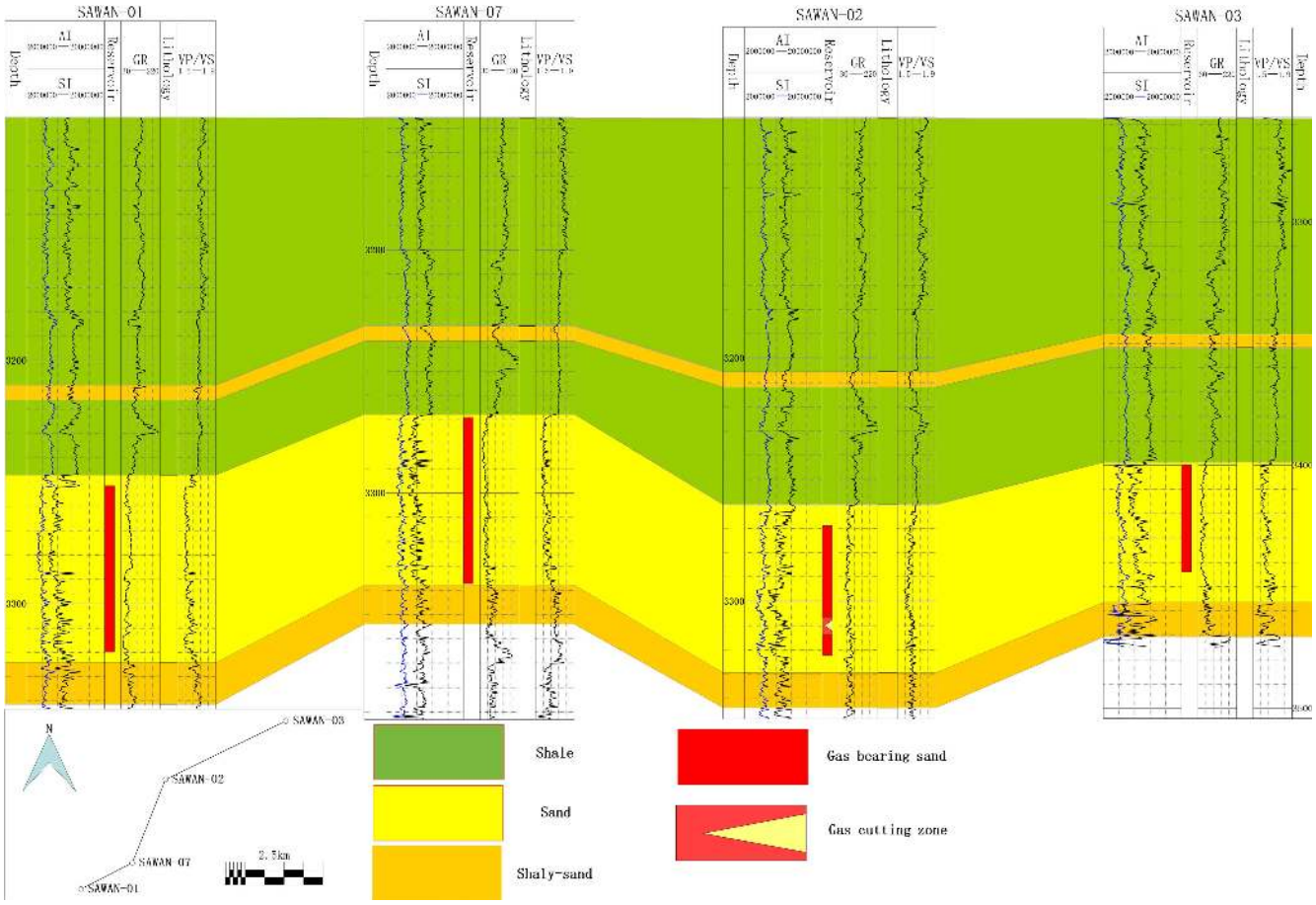

Figure 12. Cross correlation of gamma ray and elastic properties of four offset wells representing the lateral and vertical variation in the reservoir zone (units of acoustic and shear impedance are Kg/m2*S, Gamma ray gAPI, and depth in meters).

(figure 11). The cross plots of these attributes clearly separates the data points into three types of clusters. The cluster having low water saturation, acoustic impedance, and shear impedance values represents gas-bearing sand. However, the cluster having high water saturation (100% saturation), acoustic impedance, and shear impedance values represents shale bodies with no gas saturation. The separation between these two clusters (sand and shale) represents water saturation (figure 11). The water-bearing sediments exhibit higher values of acoustic impedance and water saturation as compared to gas-bearing sediments. These water-bearing sediments can also be clearly identified on the cross plots having elastic and water saturation values between gas-bearing sand and shale bodies. On the basis of petrophysical and cross-plot analysis, the average quantitative (cutoff) values of elastic and petrophysical properties for different rock types have been defined (table 2). The cross-plotting results show that our calibrated model effectively predicts the lithology and fluid content in the Sawan gas field, Middle Indus Basin, Pakistan.

In order to develop a good understanding of the geometry, depositional setting, and continuity of different stratigraphic units encountered in different wells in the same area, well correlation is performed. Therefore, to analyze the lateral and vertical variations in the marked stratigraphic units encountered in the four wells (Sawan-01, -02, -03, and -07), the logs of P-wave impedance, S-wave impedance, gamma ray, and V_P/V_S ratio are plotted together for all four wells. For this purpose, interpolation between wells was performed. Four wells (Sawan-01, -02, -03, and -07) have been used to analyze the litho-fluid behavior of the reservoir. The upper thick shale of Lower Goru Formation is considered as a datum plane. A SW–NE trending cross section (figure 12) through four wells shows the correlation between calculated lithologies. Figure 12 shows that the upper part of the Lower Goru Formation is composed of thick shale intervals with interbedded thin intervals of shaly sand, and the lower part of the formation is mainly composed of reservoir-quality sand with a shaly sand interval at the bottom. The analysis indicates that this sand interval is a gas-bearing reservoir in the study area. The thickness of shale increases from the SW to NE direction, whereas thickness of reservoir-quality sand decreases in this direction. In this area, Khairpur High plays an important role in controlling the reservoir quality and stratigraphic traps (Ahmad and Chaudhry 2002). The uplifting of Khairpur High positioned the Lower Goru reservoir-quality sand of proximal depositional system in structurally deep areas. While non-reservoir-quality shale and shaly sands are positioned updip to form traps (Berger *et al* 2009), Sawan-02 well shows reservoir compartmentalization and has relatively poor reservoir character; this is due to the relatively

proximal location of the Sawan-02 well to Khairpur High compared to other wells.

5. Conclusions

In this study, an integrated petrophysical and rock physics modeling approach is adopted to understand the reservoir characterization of the Lower Goru Formation in the Sawan Gas Field of the Middle Indus Basin, Pakistan. The developed methodology helped us to build up an accurate and consistent rock physics model. The calibrated model shows good consistency between measured and modeled velocities. The correlation between measured and modeled P and S wave velocities is 92.76% and 84.99%, respectively (figure 7). The good consistency of the model laid a significant foundation for improved reservoir characterization in the study area. The calibrated model has also proven helpful in accurately estimating the elastic parameters (density, P and S wave velocities) even in those wells (Sawan-02) where both sonic and shear logs were missing in the target zones. Cross plots of these calculated parameters clearly delineate the lithology and fluid content. On the basis of these cross plots, the quantitative values (average cutoff values) of elastic and petrophysical parameters have been defined in order to discriminate between the gas-bearing sand, shale, and shaly sand zones. It is found that *the* V_P/V_S ratio is more sensitive to gas-bearing sand followed by acoustic impedance. Lateral and vertical variation in the reservoir is analyzed through cross-correlation methodology. The correlation shows that thickness of shale increases whereas quality of sand decreases from the SW to NE direction. The proposed model allows for accurate discrimination between different types of facies and provides quick results. It can also be effectively utilized in seismic inversion to improve seismic reservoir characterization.

Acknowledgments

The authors would like to express their appreciation to the Directorate General of Petroleum Concession (DGPC), Pakistan for the release of data used in this study. We extend our appreciation to the China Scholarship Council for providing us a chance to enhance our research abilities. We are also thankful to Mr Shafiq-ur-Rehman (meteorologist at Pakistan Meteorological Department, Islamabad, Pakistan) and our labmates working in the Geodetection Lab of China University of Geosciences, Beijing for their valuable suggestions and fruitful discussions.

References

Adeoti L, Ayolabi E A and James P L 2009 An integrated approach to volume of shale analysis: Niger Delta example, offshore field *World Appl. Sci. J.* **7** 448–52

Ahmad N and Chaudhry S 2002 Kadanwari gas field, Pakistan: a disappointment turns into an attractive development opportunity *Petrol. Geosci.* **8** 307–16

Ahmed N, Fink P, Sturrock S, Mahmood T and Ibrahim M 2004 Sequence stratigraphy as predictive tool in Lower Goru Fairway, Lower and Middle Indus Platform, Pakistan *Pakistan Association of Petroleum Geoscientist (PAPG), Annual Technical Conference (ATC)* 85–104

Ahmed N, Khalid P and Anwar A W 2016 Rock physics modeling to assess the impact of spatial distribution pattern of pore fluid and clay contents on acoustic signatures of partially-saturated reservoirs *Acta Geod. Geophys.* **51** 1–13

Ajisafe Y C and Ako B D 2013 3D seismic attributes for reservoir characterization of 'Y' field Niger Delta, Nigeria IOSR *J. Appli. Geol. Geophys.* **1** 23–31

Alao P A, Ata A I and Nwoke C E 2013 Subsurface and petrophysical studies of shaly-sand reservoir targets in Apete field, Niger Delta *ISRN Geophys.* **2013** 102450

Avseth P 2000 Combining rock physics and sedimentology for seismic reservoir characterization of North Sea turbidite systems *PhD Thesis* Stanford University, CA

Avseth P and Bachrach R 2005 Seismic properties of unconsolidated sands: tangential stiffness, Vp/Vs ratios and diagenesis *75th Annual Meeting SEG Expanded Abstracts* pp 1473–6

Avseth P, Mukerji T and Mavko G 2005 *Quantitative Seismic Interpretation–Applying Rock Physics Tools to Reduce Interpretation Risk* (Cambridge: Cambridge University Press)

Avseth P, Mukerji T, Jorstad A, Mavko G and Veggeland T 2001 Seismic reservoir mapping from 3D AVO in a North Sea turbidite system *Geophys. Soc. Expl. Geophys.* **66** 1157–76

Batzle M L and Wang Z 1992 Seismic properties of fluids *Geophysics* **57** 1396–408

Benzing W M, Byerly P E and Hopkins J R 1983 Shear and compressional wave data interpretation—Midland basin, Texas *53rd SEG Annual Meeting, Las Vegas Expanded Abstracts* pp 358–9

Berger A, Gier S and Krois P 2009 Porosity-preserving chlorite cements in shallow–marine volcanic clastic sandstones: evidence of the Sawan gas field, Pakistan *AAPG Bulletin* **93** 595–615

Berryman J G 1980 Long-wavelength propagation in composite elastic media *J. Acoust. Soc. Am.* **68** 1809–31

Beryman J G and Milton G W 1991 Exact results for generalized Gassmann's equations in composite porous media with two constituents *Geophysics* **56** 1950–60

Bisht B S, Sas S K, Chaudhuri P K, Singh R B N and Singh S K 2013 Integration of petrophysics & rock-physics modeling in single workflow reduces uncertainty in seismic reservoir characterization: a case study *Geohorizons* 44–7

Brie A, Pampuri F, Marsala A F and Meazza O 1995 Shear sonic interpretation in gas bearing sands *SPE Annual Technical Conference and Exhibition* SE-30595-MS

Carmichael R S 1989 *Practical Handbook of Physical Properties of Rocks and Minerals* (Boca Raton, FL: CRC Press)

Castagna J P and Swan H W 1997 Principles of AVO crossplotting *Lead. Edge* **17** 337–42

Castagna J P, Batzle M L and Kan T K 1993 Rock physics—the link between rock properties and AVO response *Offset-Dependent Reflectivity–Theory and Practice of AVO Analysis* (Tulsa, OK: Society of Exploration Geophysicists) vol 8, pp 135–71

Cheng C H and Toksöz M N 1979 Inversion of seismic velocities for the pore aspect ratio spectrum of a rock *J. Geophys. Res.* **84** 7533–43

Chi X and Han D 2009 Lithology and fluid differentiation using rock physics templates *Lead. Edge* **28** 60–5

Clavier C, Hoyle W and Meunier D 1971 Quantitative interpretation of thermal neutron decay time logs: I. Fundamentals and techniques *J. Petrol. Technol.* **23** 743–55

Doveton H 1999 *Basic Oil and Gas Log Analysis* Kansas Geological Survey USA 8–16
Dvorkin J and Nur A 1996 Elasticity of high-porosity sandstones, theory for two North Sea data sets *Geophysics* **61** 559–64
Dvorkin J, Nur A and Yin H 1994 Effective properties of cemented granular material *Mech. Master* **18** 351–66
Eshelby J D 1957 The determination of the elastic field of an ellipsoidal inclusion and related problems *Proc. R. Soc. Lond. Ser.* A **241** 376–96
Feng-Ying Y, Xing-Yao Y and Bo L 2014 S-wave velocity self-adaptive prediction based on a variable dry rock frame equivalent model *J. Geophys. Eng.* **11** 045015
Fitch P J, Lovell M A, Davies S J, Pritchard T and Harvey P K 2015 An integrated and quantitative approach to petrophysical heterogeneity *Mar. Pet. Geol.* **63** 82–96
Gassmann F 1951 Uber die elastizitat poroser medien *Vier. der Natur Gesellschaft* **96** 1–23
Grana D, Pirrone M and Mukerji M 2012 Quantitative log interpretation and uncertainty propagation of petrophysical properties and facies classification from rock-physics modeling and formation evaluation analysis *Geophysics* **77** 45–63
Hamada G M 1996 An integrated approach to determine shale volume and hydrocarbon potential in shaly sand *Presented at SCA Int. Symp.* 2093–107
Hashin Z and Shtrikman S 1963 A variational approach to the elastic behavior of multiphase materials *J. Mech. Phys. Solids* **11** 127–40
He F B, You J and Chen K Y 2011 Gas sand distribution prediction by elastic inversion based on rock physics modelling and analysis *Appl. Geophys.* **8** 197–205
Hill R 1952 The elastic behaviour of a crystalline aggregate *Proc. Phys. Soc. London* **65** 349–54
Hu R Y, Holden T and Broussard M 2011 Petrophysics and rock physics modeling to improve seismic reservoir characterization —case study of lower hackberry sandstone *AAPG Annual Convention and Exhibition (Houston, Texas, USA)* Article # 40774
Hughes P, Eykenhof V R and Mesdag P 2008 *Estimation of Hydrocarbons in-Place by Simultaneous (AVO) Inversion, Constrained by Iteratively Derived Low Frequency Models* (Stavanger, Norway: Fugro-Jason)
Hussein R A and Ahmed M E B 2012 Petrophysical evaluation of shaly sand reservoirs in Palouge-Fal oilfield, Melut Basin, South East of Sudan. Engineering and computer sciences (ECS) *J. Sci. Technol.* **13** 2
Iqbal M W A and Shah S M I 1980 *A A Guide to the Stratigraphy of Pakistan* 53 (Geological Survey of Pakistan)
Kadri I B 1995 *Petroleum Geology of Pakistan* 1st edn (Karachi, Pakistan: Pakistan Petroleum Ltd)
Kazmi A H and Jan M Q 1997 *Geology and Tectonics of Pakistan* 1st edn (Karachi, Pakistan: Graphic Publishers)
Khalid P, Ahmed N, Naeem M and Khan K A 2014 A modeling study of AVO-derived attributes to differentiate reservoir facies from non-reservoirs facies and fluid discrimination in Penobscot area, Nova Scotia *Geosci. J.* **19** 471–80
Khalid P, Broseta D, Nichita D V and Blanco J 2014(b) A modified rock physics model for analysis of seismic signatures of low gas-saturated rocks *Arab. J. Geosci.* **7** 3281–95
Khalid P, Ahmed N, Mahmood A and Saleem M A 2016 An integrated seismic interpretation and rock physics attribute analysis for pore fluid discrimination *Arab. J. Sci. Eng.* **41** 191–200
Krois P, Mahmood T and Milan G 1998 Miano Field, Pakistan, a case history of model driven exploration *Proc. Pakistan Petroleum Convention, Pakistan Assoc. Petroleum Geologists, Islamabad* pp 111–31
Kuster G T and Toksoz M N 1974 Velocity and attenuation of seismic waves in two-phase media: 1. Theoretical formulation *Geophysics* **39** 587–606
Larionov V V 1969 *Radiometry of Boreholes (in Russian)* (Moscow: Nedra)
Liu Z S and Sun S Z 2015 The differential Kuster–Toksöz rock physics model for predicting s-wave velocity *J. Geophys. Eng.* **12** 839
Marion D, Nur A, Yin H and Han D 1992 Compressional velocity and porosity in sand–clay mixtures *Geophys.* **57** 554–63
Mavko G, Mukerji T and Dvorkin J 1998 *The Rock Physics Handbook; Tools for Seismic Analysis in Porous Media* 1st edn (New York: Cambridge University Press)
Mavko G, Mukerji T and Dvorkin J 2009 *The Rock Physics Handbook; Tools for Seismic Analysis of Porous Media* 2nd edn (New York: Cambridge University Press)
McPhee C A and Enzendorfer C K 2004 Sand management solutions for high-rate gas wells, Sawan field, Pakistan *SPE International Symposium and Exhibition on Formation Damage Control* 94–103
Mindlin R D 1949 Compliance of elastic bodies in contact *J Appl. Mech.* **16** 259–68
Minear M J 1982 Clay models and acoustic velocities *57th Annual Meeting American Institute of Mining and Metallurgical Engineers (New Orleans)* Paper 11031-MS SPE
Munir K, Iqbal M A, Farid A and Shabih S M 2011 Mapping the productive sands of Lower Goru Formation by using seismic stratigraphy and rock physical studies in Sawan area, southern Pakistan: a case study *J. Petrol. Explor. Prod. Technol.* **1** 33–42
Odegaard E and Avseth P 2004 Well log and seismic data analysis using rock physics templates *First Break* **23** 37–43
Poupon A and Gaymard R 1970 The evaluation of clay content from logs *SPWLA 11th Annual Logging Symp. Conf.* Paper 1970-G
Poupon A and Levaux J 1971 Evaluation of water saturation in shaly formations *Society of Professional Well Log Analysts 12th Annual Logging Symp. Transactions* paper SPWLA-1971-vXIIn4a1
Reuss A 1929 Berechnung der fliessgrense von mischkristallen auf grund der plastizitatbedingung fur einkristalle *Zeitschrift fur Ange-Wandte Mathematikaus Mechnik* **9** 49–58
Sams M 2014 Constraining petrophysics with rock physics *EAGE/FESM Joint Regional Conf. Petrophysics Meets Geoscience (Kuala Lumpur, Malaysia)*
Sams M S and Andrea M 2001 The effect of clay distribution on the elastic properties of sandstones *Geophys. Prospect.* **49** 128–50
Sams M S and Focht T 2013 An effective inclusion-based rock physics model for a sand–shale sequence *First Break* **31** 61–71
Schlumberger Limited 1974 *Log Interpretation: Applications* 2
Stieber S J 1970 Pulsed Neutron Capture Log Evaluation— Louisiana Gulf Coast Society of Petroleum Engineers (https://doi.org/10.2118/2961-MS)
Voigt W 1910 *Lehrbuch der Kristallphysik* (Leipzig: Teubner)
Walls J, Dvorkin J and Carr M 2004 Well logs and rock physics in seismic reservoir characterization *Offshore Technology Conf. Offshore Technology Conf.*
Walton K 1987 The effective elastic moduli of a random packing of spheres *J. Mech. Phys. Solids* **35** 213–26
Wandrey C J, Law B E and Shah H A 2004 *Sembar Goru/Ghazij composite total petroleum system, Indus and Sulaiman-Kirthar geologic provinces, Pakistan and India (No. 2208-C)*
Wang Q, Wang Y, Guo S G, Xing S T and Liu Z W 2015 The effect of shale properties on the anisotropic brittleness criterion index from laboratory study *J. Geophys. Eng.* **12** 866
White R E 1991 Properties of instantaneous seismic attributes *Lead. Edge* **10** 26–32
Widarsono B 2012 Choice of water saturation model in log analysis and its implication to water saturation estimates–a further investigation *Sci. Contrib. Oil Gas* **35** 3
Wyllie M R J, Gregory A R and Gardner L W 1956 Elastic wave velocities in heterogeneous and porous media *Geophysics* **21** 41–70

Xu S and Payne M A 2009 Modelling elastic properties in carbonate rocks *Lead. Edge* **28** 66–74

Xu S and White R E 1995 A new velocity model for clay-sand mixtures *Geophys. Prospect.* **43** 91–118

Yuedong Q and Hongwei A 2007 Study of petrophysical parameter sensitivity from well log data *Appl. Geophys.* **4** 282–7

Zhang Z 2008 A rock physics model for hydrates bearing sediments of near surface *SEG Las Vegas Annual Meeting* pp 1799–803

Zhao L, Geng J, Han D H, Cheng J and Guo T 2013 Rock physics based probabilistic lithology and fluid prediction in a heterogeneous carbonate reservoir *Annual SEG Meeting Houston (USA)* pp 2387–91 (http://dx.doi.org/10.1190/segam2013-0486.1)